Observations of Extreme Temperature and Wind Gradients near the Summer Mesopause during the MaCWAVE/MIDAS Rocket Campaign

D. C. Fritts and B. P. Williams[1]
Colorado Research Associates, a division of Northwest Research Associates, Boulder, Colorado

C. Y. She and J. D. Vance
Department of Physics, Colorado State University, Fort Collins, Colorado

M. Rapp, F.-J. Lübken, and A. Müllemann
Leibniz Institute of Atmospheric Physics, Kühlungsborn, Germany

F. J. Schmidlin
NASA/Wallops Flight Facility, Wallops Is., VA

R. A. Goldberg
NASA/Goddard Space Flight Center, Greenbelt, MD

Abstract.
We present measurements of extremely large gradients of temperature and zonal wind near and above the arctic summer mesopause obtained with sodium lidar and in situ rocket instrumentation during the MaCWAVE/MIDAS rocket and ground-based measurement campaign performed at the Andøya Rocket Range (ARR) and the ALOMAR observatory (69.3°N, 16.0°E) in July 2002. The gradients appear to result from strong gravity wave forcing of the summer mesopause, vertical scale compression and amplitude increases accompanying increasing stratification and decreasing intrinsic phase speeds, and the turbulent transport accompanying wave instability in the lower thermosphere. Zonal wind gradients are found to exceed 100 m s^{-1} km^{-1}, while temperature gradients range from superadiabatic to ∼40 to 100 K km^{-1}. We also explore the implications of these large gradients for further instability of the gravity wave and mean fields.

Introduction

It is now well known that gravity wave dissipation and momentum flux divergence account for closure of the mesospheric jets and an induced residual circulation from the summer to the winter hemisphere near the mesopause [*Holton*, 1982; *Nastrom et al.*, 1982; *McIntyre*, 1989; *Fritts and Yuan*, 1989; *Fritts and Alexander*, 2003]. The induced mean vertical motion of ∼0.05 m s^{-1} near the summer mesopause cools the upper mesosphere to ∼130 K, approximately 90 K colder than radiative equilibrium conditions [*Garcia*, 1989; *Lübken and von Zahn*, 1991; *Fritts and Luo*, 1995]. The resulting thermal structure approaches adiabatic in the upper mesosphere and is highly stratified in the lower thermosphere, implying large vertical wavelengths and a weaker tendency for gravity wave instability below the mesopause, but constricted vertical wavelengths and stronger dissipation and drag above [*VanZandt and Fritts*, 1989]. Downward transport of heat accompanying wave instability and turbulence in the lower thermosphere likely contributes to the large mean thermal gradients above the mesopause. Because the mesopause thermal structure is wave driven, it also exhibits variability with the strength of wave forcing.

Wind gradients observed during the summer MaCWAVE/MIDAS rocket salvoes are comparable to the largest seen in over 400 chemical release measurements at many locations (including high latitudes) over four decades, and are larger than all but one measurement below ∼100 km [*Larsen*, 2002]. Temperature gradients are likewise among the largest observed above the planetary boundary layer, but are comparable to previous high-resolution measurements at these altitudes [*Rapp et al.*, 2002]. As such, the gradients measured near the mesopause at ARR and ALOMAR may be characteristic of the summer polar mesopause environment, and the dynamics underlying them warrants further investigation.

The discussion here focuses on measurements obtained during the summer MaCWAVE/MIDAS rocket salvoes performed in July 2002 with ground-based and in situ instrumentation (see *Goldberg et al.* [2004], this issue, for an overview). Our thesis is that very large temperature and wind gradients above the mesopause, and evidence of larger than usual fluctuations below the mesopause, are indicative of stronger than normal gravity wave forcing and variations in the altitudes at which this forcing occurs, for which additional evidence during the summer rocket salvoes is offered by *Goldberg et al.* [2004], *Rapp et al.* [2004], and *Becker et al.* [2004] in this issue.

This paper is organized as follows. A brief description of the relevant instrumentation is provided in Section 2. Section 3 displays the evidence for and characteristics of large temperature and wind gradients near and above the mesopause. Our interpretation of these results and our conclusions are provided in Sections 4 and 5.

[1] also with Department of Physics, Colorado State University, Fort Collins, Colorado

Paper number .
0094-8276/04/$5.00

Instrumentation

The instrumentation employed to explore the structure of large temperature and wind gradients occurring near the arctic summer mesopause represents a small subset of those employed for the summer MaCWAVE/MIDAS rocket and ground-based measurement campaign. Here we use data only from the Weber sodium lidar at ALOMAR [*She et al.*, 2002], falling spheres aboard Viper MET rockets [*Schmidlin et al.*, 1991], and the CONE instrument aboard the MIDAS sounding rocket [*Blix et al.*, 2003], the capabilities of which are described briefly below. A more complete description of the campaign and of the observed mean state during summer 2002 is provided by *Goldberg et al.* [2004].

a. Weber sodium lidar

The Weber sodium lidar is an advanced resonance lidar achieving narrow-band, three-frequency measurements of radial winds and temperatures near the summer mesopause via sum-frequency generation of 589 nm light at the D2a sodium peak, acousto-optic frequency shifting to the wings of the D2a line, and Faraday filters in the data acquisition system to permit full daytime measurement capabilities. During the summer rocket campaign, the Weber lidar measured radial winds and temperatures employing the ALOMAR 1.8-m telescopes inclined 20^o to the east and west. To provide sensitivity to large gradients in a dynamically very active environment with low sodium densities, lidar data were acquired at 150-m and 1-min resolution and averaged for 1 hr. A Hamming window having an effective vertical smoothing of 1 km was employed to reduce uncertainties in radial wind and temperature estimates due to photon statistics.

b. CONE

The CONE ionization gauge aboard the MIDAS payload during each summer salvo measured atmospheric density and enabled determination of temperature (assuming hydrostatic equilibrium) with ∼200-m resolution and a 2% (∼3 K) uncertainty below ∼95 km [*Giebeler et al.*, 1993; *Rapp et al.*, 2001]. Only those data obtained during the first salvo are employed here, however, because of coning of the payload on descent during the second MIDAS flight. The flight track for the MIDAS payload was towards the northwest, yielding downleg measurements ∼30 km north of the west beam (at 20^o zenith angle) of the Weber sodium lidar at a 90-km altitude. Additional information on the CONE instrument and its application to turbulence measurements during the first MaCWAVE/MIDAS salvo are provided by *Rapp et al.* [2004].

c. Falling spheres

During the summer MaCWAVE/MIDAS salvoes, 26 falling spheres were launched by Viper and Super-Loki rocket motors and tracked with a mobile, high-precision, C-band tracking radar. Estimates of temperatures and winds were made using third-degree Legendre polynomial fits to the horizontal and vertical position and velocity data. Effective filter lengths for these data were ∼ 10 to 12 km for densities (temperatures) and winds above ∼ 80 km, decreasing to 5, 3, and 1 km at 70, 60, and 40 km altitude, respectively. Because wind filters are somewhat coarser than density/temperature filters above ∼ 80 km, however, we employ only the temperature data in this paper. Additional details on the falling sphere method are provided by *Schmidlin et al.* [1991] and *Müllemann* [2003].

Evidence for Extreme Mesopause Gradients of Wind and Temperature

We begin by displaying profiles of temperature and zonal wind inferred with the Weber lidar and falling spheres for the two salvoes on 1/2 and 4/5 July 2002 in Figures 1 and 2. Lidar profiles are

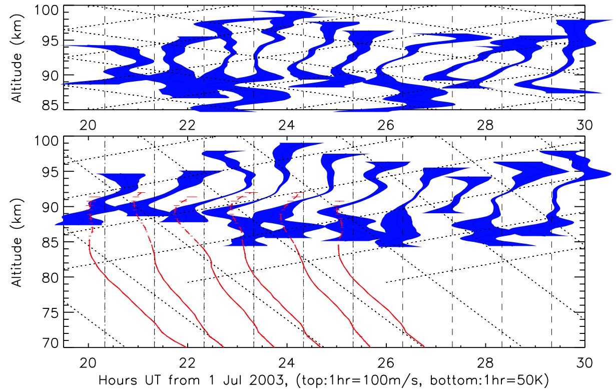

Figure 1. Winds (top) and temperatures (bottom) measured with the west beam of the Weber sodium lidar (with error bars due to photon statistics) and by falling spheres aboard the Viper MET rockets (bottom panel, with solid lines below 85 km and dashed lines with error bars above) at hourly intervals during Salvo 1 of the MaCWAVE/MIDAS rocket campaign on 1/2 July 2002. Weber lidar measurements were averaged for 1 hr and smoothed with a 1-km Hamming window. Diagonal lines show gradients of ± 100 m $s^{-1}km^{-1}$ (top panel) and -9.5 and +40 K km^{-1} (bottom panel).

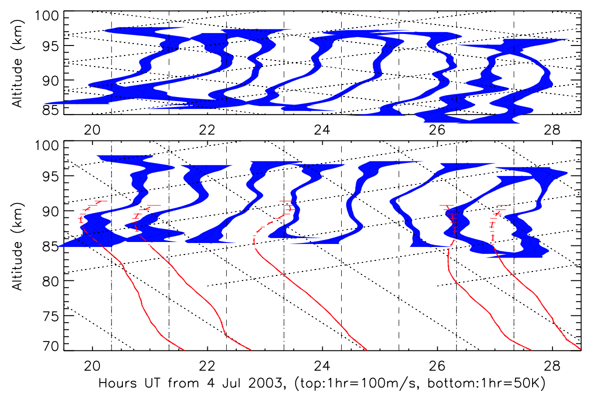

Figure 2. As in Figure 1, but for MaCWAVE/MIDAS Salvo 2 on 4/5 July 2002.

for the west beam data only, given its greater photon counts and proximity to the falling sphere data. These data reveal large and variable gradients of temperatures and winds, with occasional large variations on time scales of 1 hr. In most cases, there appear to be correlations between the wind and temperature fluctuations in the lidar data suggestive of gravity waves having vertical wavelengths of ∼2 to 5 km or greater superposed on the positive mean gradients of zonal wind and temperature above ∼87 km. There are also suggestions of significant gradients in falling sphere temperatures, though the altitudes at which the extreme gradients occur are at the limits of the falling sphere technique. We are confident of the low-pass temperature profiles to 85 km. At greater altitudes (shown with horizontal error bars above 85 km for the Viper falling spheres in the lower panels of Figures 1 and 2), the structures are suggestive of merging with lidar data above, but are strongly smoothed in altitude because of the slow sphere response where densities are very small.

While the largest temperature gradients are positive because of the positive mean gradients at greater altitudes, there are nevertheless large negative gradients as well. These often exceed the adiabatic lapse rate in the temperature field (-9.5 K km^{-1}, shown at

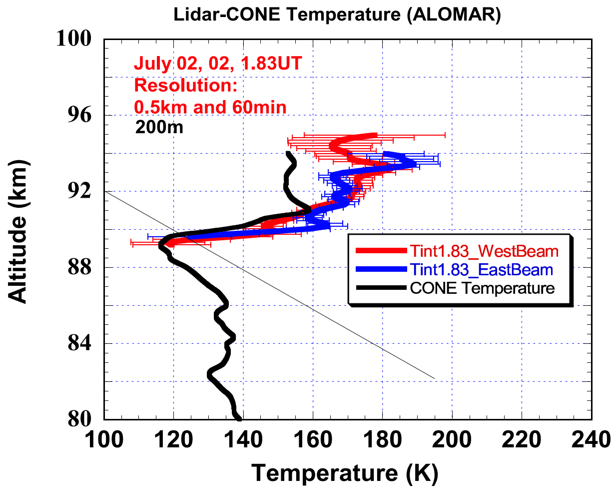

Figure 3. Temperature profiles obtained with the east (blue) and west (red) beams of the Weber lidar and the CONE instrument (black) during Salvo 1. Resolution of the lidar data in this case was 1 hr and 0.5 km. Resolution of the CONE instrument at these altitudes was $\sim$ 100 m. The straight line shows an adiabatic lapse rate for reference.

the lower left in each panel) and suggest gravity wave overturning and turbulence generation below and above the mesopause. In particular, significant wind and temperature gradients at small vertical wavelengths and the differences between east- and west-beam lidar measurements (see below) imply gravity waves having large amplitudes, small intrinsic phase speeds, and horizontal wavelengths of tens of km.

Further confirmation of large positive and negative temperature gradients comes from the CONE instrument. The CONE temperature profile is shown in Figure 3, together with east- and west-beam Weber lidar profiles averaged over 0.5 km and 1 hr and centered on the CONE measurement interval. In particular, CONE measurements agree most closely with temperatures measured in the west beam of the Weber lidar (closest to the CONE measurements), but also confirm the occurrence of near-adiabatic or super-adiabatic gradients below the mesopause. Additional and independent evidence of gravity wave instability above and below the mesopause comes from CONE turbulence intensity measurements, which reveal nearly continuous turbulence layers between $\sim$ 72- and 90-km altitudes, and the first arctic summer measurements of turbulence below $\sim$ 82 km [*Rapp et al.*, 2004].

Discussion

The extreme temperature gradients measured by the Weber lidar and CONE occurred in the presence of mean gradients during the summer salvoes that were $\sim$10 to 20 K km^{-1} over an altitude range of $\sim$89 to 92 km immediately above the mesopause. Above this enhanced mean gradient was a weaker, though not adiabatic, mean gradient over a several km altitude range above $\sim$92 km (see Figure 3 of *Goldberg et al.* [2004]). Extreme small-scale gradients in the presence of a large mean temperature gradient are expected based on the enhanced saturation theory by *VanZandt and Fritts* [1989]. The theory also suggests possible gravity wave influences on the mean temperature structure in response to enhanced wave dissipation and turbulent mixing accompanying the sharp increase in stability.

In order to estimate possible gravity wave amplitudes and effects above the mesopause, we assume a gravity wave to have constant momentum flux, $\overline{\rho u'_h w'}$, from the upper mesosphere until dissipating at greater altitudes, where $\overline{\rho}$ is mean density, u'_h and w' are the horizontal and vertical perturbation velocities in the plane of wave propagation, and the overbars denote a spatial or temporal average. Additionally, the ratio of horizontal and vertical velocities varies approximately as

$$u'_h/w' \sim m/k_h \sim N/\omega, \tag{1}$$

for a vertical wavelength $\lambda_z = 2\pi/m << 4\pi H$, where $\omega = k_h(c-\overline{u})$ is intrinsic frequency, $\lambda_h = 2\pi/k_h$ is the horizontal wavelength in the direction of wave propagation, H is the density scale height, and N is the buoyancy frequency. From the dispersion relation for hydrostatic waves, we also have

$$m \sim N/(c-\overline{u}). \tag{2}$$

Thus, m likely increases strongly as a gravity wave propagates into the more stratified lower thermosphere, both because

$$N^2 = (g/\overline{\theta})d\overline{\theta}/dz = (g/\overline{T})(d\overline{T}/dz + g/c_p) \tag{3}$$

increases with the increasing temperature gradient and because primary wave propagation in summer is eastward [*Williams et al.*, 2004] and the mean zonal wind increases with altitude around the mesopause [*Goldberg et al.*, 2004], such that $(c-\overline{u})$ decreases with altitude. Increasing m implies, from Eqs. (1) and (2) with constant momentum flux,

$$u'^2_h \sim N/\omega\overline{\rho}, \tag{4}$$

$$(du'_h/dz)^2 \sim N^3/\omega^3\overline{\rho}, \tag{5}$$

and (employing the vertical momentum equation) a nondimensional wave amplitude,

$$a = u'_h/(c-\overline{u}) = k_h u'_h/\omega \sim (d\theta'/dz)/(d\overline{\theta}/dz). \tag{6}$$

With an increase of N of $\sim$3, a decrease of $(c-\overline{u})$ of $\sim$ 2 (a conservative value inferred from largely eastward propagation at lower altitudes, intrinsic phase speeds of $\sim$ 30 m s^{-1} near 50 km, and zonal wind increases near the mesopause), and an increase in altitude of H, we anticipate that u'_h, a, and du'_h/dz will increase by $\sim$5, 10, and 20, respectively, apart from dissipation effects. Indeed, the increased gravity wave wind and temperature perturbations and gradients noted above are qualitatively consistent with these expectations and appear to support the argument for enhanced wave instability, turbulence, and turbulent mixing in response to gravity wave propagation through the summer mesopause [*VanZandt and Fritts*, 1989]. In particular, the largest wind and temperature gradients above the mesopause are $\sim$100 m s^{-1} km^{-1} and 100 K km^{-1}. With gravity wave perturbations symmetric about the mean, we infer from Figure 2 of *Goldberg et al.* [2004] and Figure 3 that mean gradients contribute at most $\sim$ 20% to large local gradients. Thus, the gradients due to gravity waves are comparable to or less than the enhancements anticipated from Eqs. (4) to (6) relative to gradients of $\sim$10 m s^{-1} km^{-1} and 10 K km^{-1} below the mesopause, likely due to instability processes constraining gravity wave amplitudes and growth rates with altitude.

Finally, we examine the evidence for both enhanced and reduced mean temperature gradients in response to strong gravity wave forcing above the mesopause. If the theory of *VanZandt and Fritts* [1989] is valid, then we anticipate a region above the mesopause in which those gravity waves having the largest amplitudes, vertical group velocities, and energy fluxes exhibit especially strong dissipation due to the amplitude enhancements noted above. This region will have a depth of $\sim$ a vertical wavelength of the dominant vertical motions, ∼10 km, and will exhibit enhanced turbulence and mixing accompanying the vertical scale compression and wave instability due to the increasing mean stratification and zonal wind shear. In fact such turbulence intensities were observed in this environment (see Figure 1 of *Rapp et al.* [2004]). The result is expected to be a strong, localized downward turbulent heat flux. Heat flux convergence below the strong turbulence will yield an enhancement of the positive mean temperature gradient inducing wave amplification and instability, while heat flux divergence above will reduce the mean temperature gradients at those altitudes. Indeed, the mean and individual temperature profiles observed in Figure 3 exhibit exactly this behavior and appear to support these arguments.

While gravity waves clearly achieve overturning amplitudes near the mesopause for the reasons discussed above, we anticipate that a variety of instabilities may be possible because of the potential for shear and buoyancy sources of turbulent energy as well as wave-wave interactions due to large wave amplitudes [*Fritts and Alexander*, 2003]. At larger vertical scales, we expect that convective instabilities will contribute most to instability and turbulence generation based on numerical studies in sheared and unsheared environments [*Andreassen et al.*, 1998; *Fritts et al.*, 2003]. At smaller vertical scales (and lower intrinsic frequencies), however, mean and wave shears likely play an increasing role, and Kelvin-Helmholtz (KH) shear instability is also expected.

Summary and Conclusions

Wind and temperature gradients observed near the arctic summer mesopause during the July 2002 summer MaCWAVE/MIDAS rocket salvoes were among the largest ever observed in the mesosphere and lower thermosphere. We have argued that such extreme temperature and wind gradients near the summer mesopause arise in response to especially strong gravity wave activity and increasing wave amplitudes and shears, turbulence generation, and turbulent transport of heat accompanying wave propagation into the highly-stratified lower thermosphere. Gradients increasing from $\sim$10 K km^{-1} and 10 m s^{-1} km^{-1} to $\sim$100 K km^{-1} and 100 m s^{-1} km^{-1} are anticipated to accompany an increasing buoyancy frequency and decreasing intrinsic frequency for waves penetrating into the lower thermosphere. Enhanced instability, in turn, leads to enhanced downward heat transport and greater stratification below and lesser stratification above this region, in accordance with theory [*VanZandt and Fritts*, 1989]. Indeed, a very similar response is also seen immediately above the tropopause extending over smaller vertical scales [*Goldberg et al.*, 2004].

The extreme gradients discussed here occur in the context of an unusual summer mesopause circulation and structure. *Goldberg et al.* [2004], *Becker et al.* [2004], and *Rapp et al.* [2004] have all revealed aspects of the 2002 summer mesopause that depart in important respects from previous years and measurements. So it should not be surprising that the mesopause gravity wave activity also differs from previous years. Indeed, this might be expected with a warmer and more stable upper mesosphere that may admit a larger fraction of the gravity wave spectrum to higher altitudes. What is not known at this stage is why larger amplitudes and turbulence intensities should accompany a weaker mean zonal forcing and residual circulation than in a more normal year. However, the mean state during Salvo 1 may itself differ in some respects from the 2002 mean state discussed by *Goldberg et al.* [2004] and *Becker et al.* [2004].

The sources of the gravity waves observed during the MaCWAVE/MIDAS campaign are not known, but may include convection, frontal activity, and wind shear [*Fritts and Alexander*, 2003], as gravity waves arising from these sources may propagate considerable distances. Gravity waves arising from orography are unlikely to contribute to the observed wave field because of zonal and meridional wind reversals at lower altitudes.

Acknowledgments. This research was supported by NASA under contracts NAS5-01075 and NAG5-02036, AFOSR under contracts F49620-00-C-0008 and F49620-03-C-0045, and NSF under grants ATM-0137354 and ATM-0137555.

References

Andreassen, O., P. O. Hvidsten, D. C. Fritts, and S. Arendt, 1998: Vorticity dynamics in a breaking gravity wave, 1. Initial instability evolution, *J. Fluid Mech.*, **367**, 27-46.

Becker, A. Müllemann, F.-J. Lübken, H. Körnich, P. Hoffmann, and M. Rapp, 2004: Modulation of the general circulation of the MLT by high Rossby-wave activity in austral winter 2002, *Geophys. Res. Lett.*, this issue.

Blix, T. A., J. K. Bekkeng, R. Latteck, F.-J. Lübken, M. Rapp, A. Schöch, W. Singer, B. Smiley, and B. Strelnikov, 2003: Rocket probing of PMSE and NLC: Results from the recent MIDAS/MaCWAVE campaign, *Adv. Space Res.*, **31**, 2061-2067.

Fritts, D. C., and M. J. Alexander, 2003: Gravity dynamics and effects in the middle atmosphere, *Rev. Geophys.*, **41**, doi:10.1029/2001RG000106.

Fritts, D. C., C. Bizon, J. A. Werne, and C. K. Meyer, 2003: Layering accompanying turbulence generation due to shear instability and gravity wave breaking, *J. Geophys. Res.*, April issue.

Fritts, D. C., and Z. Luo, 1995: Dynamical and radiative forcing of the summer mesopause circulation and thermal structure, 1. Mean solstice conditions, *J. Geophys. Res.*, **100**, 3119-3128.

Fritts, D. C., and L. Yuan, 1989: Measurement of momentum fluxes near the summer mesopause at Poker Flat, Alaska, *J. Atmos. Sci.*, **46**, 2569-2579.

Giebeler, J., and F.-J. Lübken and M. Nägele, 1993: CONE - a new sensor for in-situ observations of neutral and plasma density fluctuations, Proc. of the 11th ESA Symp. on European Rocket and Balloon Programmes and Related Research, Montreux, Switzerland, ESA-SP-355, 311-318.

Goldberg, R. A., D. C. Fritts, B. P. Williams, C.-Y. She, D. A. Krueger, F.-J. Lübken, W. Singer, R. Latteck, P. Hoffman, A. Müllemann, F. J. Schmidlin, and C. Mertens, 2004: The MaCWAVE/MIDAS rocket and ground-based measurement of polar summer dynamics: Overview and mean state structure, *Geophys. Res. Lett.*, this issue.

Holton, J. R., 1982: The role of gravity wave-induced drag and diffusion in the momentum budget of the mesosphere, *J. Atmos. Sci.*, **39**, 791-799.

Larsen, M. F., 2002: Winds and shears in the mesosphere and lower thermosphere: Results from four decades of chemical release wind measurements, *J. Geophys. Res.*, **107**, 10.1029/2001JA000218.

Lübken, F.-J., and U. von Zahn, 1991: Thermal structure of the mesopause region at polar latitudes, *J. Geophys. Res.*, **96**, 20,841-20,857.

McIntyre, M.E., 1989: On dynamics and transport near the polar mesopause in summer, *J. Geophys. Res.*, **94**, 14,617-14,628.

Müllemann, A., Temperaturen, Winde und Turbulenz in der polaren Sommermesosphaere, Ph.D. thesis, University of Rostock, 2003.

Nastrom, G. D., B. B. Balsley, and D. A. Carter, 1982: Mean meridional winds in the mid- and high-latitude summer mesosphere, *Geophys. Res. Lett.*, **9**, 139-142.

Rapp. M., J. Gumbel, and F.-J. Lübken, 2001: Absolute density measurements in the middle atmosphere, *Ann. Geophys.*, **19**, 571-580.

Rapp, M., F.-J. Lübken, A. Müllemann, G. E. Thomas, and E. J. Jensen, 2002: Small-scale temperature variations in the vicinity of NLC: Experimental and model results, *J. Geophys. Res.*, **107**, doi:10.1029/2001JD001241.

Rapp, M., B. Strelnikov, A. Müllemann, F.-J. Lübken, and D. C. Fritts, 2004: Turbulence measurements and implications for gravity wave dissipation during the MaCWAVE/MIDAS summer rocket program, *Geophys. Res. Lett.*, this issue.

Schmidlin, F. J., H. S. Lee, and W. Michel, 1991: The inflatable sphere: A technique for the accurate measurement of middle atmosphere temperatures, *J. Geophys. Res.*, **96**, 22,673-22,682.

She, C. Y., Joe D. Vance, B. P. Williams, D. A. Krueger, H. Moosuller, D. Gibson-Wilde, and D. C. Fritts, 2002: Lidar studies of atmospheric dynamics near polar mesopause, *EOS Transactions*, American Geophysical Union, **83** (27), 289-293.

VanZandt, T. E., and D. C. Fritts, 1989: A theory of enhanced saturation of the gravity wave spectrum due to increases in atmospheric stability, *Pure Appl. Geophys.*, **130**, 399-420.

Williams, B. P., J. D. Vance, C.-Y. She, D. C. Fritts, L. Wang, F. J. Schmidlin, R. A. Goldberg, U.-P. Hoppe, W. Singer, and R. Latteck, 2004: Gravity waves in the MLT region during the MaCWAVE/MIDAS Summer Rocket Program, *Geophys. Res. Lett.*, this issue.

D. C. Fritts, Colorado Research Associates, 3380 Mitchell Lane, Boulder CO 80301 (dave@cora.nwra.com)

(Received ____________________.)